J|A|C|S
ARTICLES

Published on Web 03/16/2009

Reductive Half-Reaction of Aldehyde Oxidoreductase toward Acetaldehyde: A Combined QM/MM Study

Sebastian Metz, Dongqi Wang, and Walter Thiel*

Max-Planck-Institut für Kohlenforschung, D-45470 Mülheim an der Ruhr, Germany

Received July 29, 2008; E-mail: thiel@mpi-muelheim.mpg.de

Abstract: We report a combined QM/MM study on the mechanism of the reductive half-reaction of aldehyde oxidoreductase. Five possible pathways are explored concerning the binding mode of acetaldehyde and the catalytic effect of the nearby glutamic acid (Glu869), taking both possible protonation states into account. In the most favorable pathway, Glu869 participates and acts as a Lewis base to deprotonate the labile hydroxide group. This proton transfer is essential for the high activity of the enzyme toward substrate because it increases the nucleophilicity of the migrating O atom and strengthens the electrophilicity of the target C atom in the substrate. The subsequent product-forming reactions occur in two discrete steps, first nucleophilic attack and then hydride transfer, which implies that the oxidation of aldehyde is a two-electron process. A variant of this mechanism, with an additional water molecule bridging the Glu869 side chain and the substrate, has similar barriers. Judging from previous gas phase calculations and our present QM/MM data, the catalytic effect of Glu869 mainly lowers the barrier of the nucleophilic attack so that the hydride transfer becomes the rate-determining step in the reductive half-reaction.

1. Introduction

Mononuclear molybdenum enzymes[1−5] constitute a large class of enzymes possessing a pterin cofactor (see Scheme 1) which coordinates to the metal center and may have different forms in different enzymes. They are generally categorized into three families by the structural homology of the active site:[1,6] xanthine oxidase, sulfite oxidase, and DMSO reductase. Important members of the first family are aldehyde oxidoreductase (AOR), xanthine dehydrogenase (XDH), and xanthine oxidase (XO). All these enzymes catalyze the oxidation of their target substrates, aldehydes or xanthine. The mechanism of these enzymatic reactions has been studied both theoretically[7−13] and experimentally.[14−26]

Structure-based catalytic mechanisms for the reductive half-reaction have been proposed[14−17] and adopted for the xanthine oxidase family. The oxygen source consumed in the biological hydroxylation process catalyzed by xanthine oxidase is recognized experimentally to be water rather than atmospheric oxygen, and the labile O should attach to the Mo center at the proximal position prior to the single turnover.[18] It has been suggested that a proton transfer from molybdenum-bound water to the nearby glutamate activates the cofactor. The substrate then interacts with the Mo-cofactor with high stereospecificity to induce the so-called reductive half-reaction. The release of the carboxylic acid product may be assisted by the transient coordination of glutamate to the metal center which will be replaced by a new water.

Due to the participation of glutamate in the metabolism, it is conceivable that the activity of the enzyme could be affected by the pH of the environment. The pH-dependence of the XO activity toward xanthine and lumazine[19] as well as 1-methylxanthine[20] has been explored, and a Lewis base-catalyzed scheme[14,17] by the glutamate at the proximal position of the coordinated Mo-center (Glu1261 in XO and Glu869 in AOR)

(1) Hille, R. *Chem. Rev.* **1996**, *96*, 2757–2816.
(2) Hille, R. *Biochim. Biophys. Acta* **1994**, *1184*, 143–169.
(3) Hille, R. *Arch. Biochem. Biophys.* **2005**, *433*, 107–116.
(4) Sauer, P.; Frébort, I. *Biol. Plant.* **2003**, *46*, 481–490.
(5) Hille, R. *Trends Biochem. Sci.* **2002**, *27*, 360–367.
(6) Mendel, R. R. *Dalton Trans.* **2005**, 3404–3409.
(7) Bray, M. R.; Deeth, R. J. *J. Chem. Soc., Dalton Trans.* **1997**, 1267–1268.
(8) Ilich, P.; Hille, R. *Inorg. Chim. Acta* **1997**, *263*, 87–93.
(9) Voityuk, A. A.; Albert, K.; Romão, M. J.; Huber, R.; Rösch, N. *Inorg. Chem.* **1998**, *37*, 176–180.
(10) Ilich, P.; Hille, R. *J. Phys. Chem. B* **1999**, *103*, 5406–5412.
(11) Ilich, P.; Hille, R. *J. Am. Chem. Soc.* **2002**, *124*, 6796–6797.
(12) Zhang, X. H.; Wu, Y. D. *Inorg. Chem.* **2005**, *44*, 1466–1471.
(13) Amano, T.; Ochi, N.; Sato, H.; Sakaki, S. *J. Am. Chem. Soc.* **2007**, *129*, 8131–8138.
(14) Huber, R.; Hof, P.; Duarte, R. O.; Moura, J. J. G.; Moura, I.; Liu, M. Y.; LeGall, J.; Hille, R.; Archer, M.; Romão, M. J *Proc. Natl. Acad. Sci. U.S.A.* **1996**, *93*, 8846–8851.
(15) Romão, M. J.; Archer, M.; Moura, I.; Moura, J. J. G.; Legall, J.; Engh, R.; Schneider, M.; Hof, P.; Huber, R. *Science* **1995**, *270*, 1170–1176.
(16) Romão, M. J.; Rösch, N.; Huber, R. *J. Biol. Inorg. Chem.* **1997**, *2*, 782–785.
(17) Okamoto, K.; Matsumoto, K.; Hille, R.; Eger, B. T.; Pai, E. F.; Nishino, T. *Proc. Natl. Acad. Sci. U.S.A.* **2004**, *101*, 7931–7936.
(18) Hille, R.; Sprecher, H. *J. Biol. Chem.* **1987**, *262*, 10914–10917.
(19) Kim, J. H.; Ryan, M. G.; Knaut, H.; Hille, R. *J. Biol. Chem.* **1996**, *271*, 6771–6780.
(20) Sau, A. K.; Mondal, M. S.; Mitra, S. *J. Chem. Soc., Dalton Trans.* **2000**, 3688–3692.
(21) Mondal, M. S.; Mitra, S. *Biochemistry* **1994**, *33*, 10305–10312.
(22) Xia, M.; Dempski, R.; Hille, R. *J. Biol. Chem.* **1999**, *274*, 3323–3330.
(23) Greenwood, R. J.; Wilson, G. L.; Pilbrow, J. R.; Wedd, A. G. *J. Am. Chem. Soc.* **1993**, *115*, 5385–5392.
(24) Howes, B. D.; Bray, R. C.; Richards, R. L.; Turner, N. A.; Bennett, B.; Lowe, D. J. *Biochemistry* **1996**, *35*, 1432–1443.
(25) Manikandan, P.; Choi, E. Y.; Hille, R.; Hoffman, B. M. *J. Am. Chem. Soc.* **2001**, *123*, 2658–2663.
(26) Doonan, C. J.; Stockert, A.; Hille, R.; George, G. N. *J. Am. Chem. Soc.* **2005**, *127*, 4518–4522.

10.1021/ja805938w CCC: $40.75

Scheme 1. Pterin Cytosine Dinucleotide (PCD) Cofactor in AOR

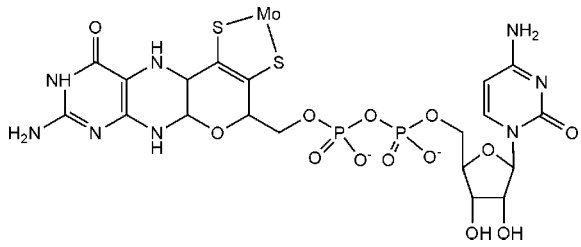

has been proposed. The experiments on temperature-dependent transient kinetics[20,21] suggest that there is at least one intermediate in the course of the turnover of xanthine to the product.

Debates on how Mo and the labile O interact with each other in the resting state have focused on three candidates: Mo−OH_2, Mo−OH, and Mo=O. The possibility of a Mo=O double bond was ruled out in an investigation that proposed a Mo−O single bond conformation[22] which is consistent with previous suggestions[23] and EPR experiments.[25] In another recent contribution, the labile O was experimentally determined by George and coworkers[26] to be a hydroxide ligand instead of a bound water molecule. In this work, an EXAFS analysis gave detailed information on the pH dependence of the Mo-cofactor conformation: the bond length of Mo−O(labile) shortens from 1.97 Å to 1.75 Å upon the increase of pH from 6 to 10. The value of 1.75 Å is in the range of Mo−O bond lengths (average: 1.77 Å) found in crystallographic databases.[27] Hence, Lewis base-assisted deprotonation is invoked to abstract a proton from Mo−OH to produce a Mo−O (or Mo=O) bond, and the labile O is assigned to be −OH.[26]

On the theoretical side, there have been a number of QM model studies that mainly focused on the oxidation of formaldehyde[7,9,12] or formamide.[10−13] In one case, acetaldehyde or formamidine were investigated as substrates.[12] The pterin cofactor (see Scheme 1) was normally modeled by a $[S-CR=CR-S]^{2-}$ ligand, R being hydrogen[7,9,10,13] or a methyl group,[11,12] so that the active species was represented by the negatively charged complex $[(S-CR=CR-S)Mo(=S)(=O)(-OH)]^-$ in most studies.[7−13] Amano et al. also considered the deprotonated and thus dianionic complex $[(S-CH=CH-S)Mo(=S)(=O)(-O)]^{2-}$, as well as a larger cofactor model.[13] None of the studies reported so far included a model for Glu869.

Two essentially different pathways have been identified, a concerted and a stepwise mechanism (see Scheme 2). For the concerted mechanism, a prohibitive barrier of 78 kcal/mol (relative to the infinitely separated reactants) was obtained in a UMP2/Lanl2DZ study with formamide as substrate.[10] Ilich and Hille[11] investigated the substituent effect of the Mo-cofactor by comparing the native form of the cofactor (sulfido) to the desulfo-form (oxo or tellurido) at the MP2 level. They found barriers for the reaction between the three congeners and formamide of 91, 78, and 75 kcal/mol for O, S, and Te, respectively, implying that the Mo=O form is inert.

An all-electron DFT(BP86) study[9] with formaldehyde as substrate located a stable intermediate prior to the hydride transfer step, which implies a stepwise mechanism. The barrier for the formation of the intermediate was not computed, while the hydride transfer was calculated to require an activation of 7.7 kcal/mol. The overall reaction was found to be thermoneutral, and hence suggested to be reversible.

The most complete study at the DFT(B3LYP) level of theory was reported by Zhang and Wu.[12] Two possible pathways, concerted and stepwise, were investigated for the reaction with the substrate formaldehyde. For the stepwise pathway, a nucleophilic attack happens first to form the O(labile atom)−C(substrate) bond followed by a hydride transfer step with cleavage of the C−H and formation of the S−H bond. The barriers for the two steps were calculated to be 17.8 and 5.4 kcal/mol, respectively. For the

Scheme 2. Mechanisms Considered in Previous Theoretical Work[a]

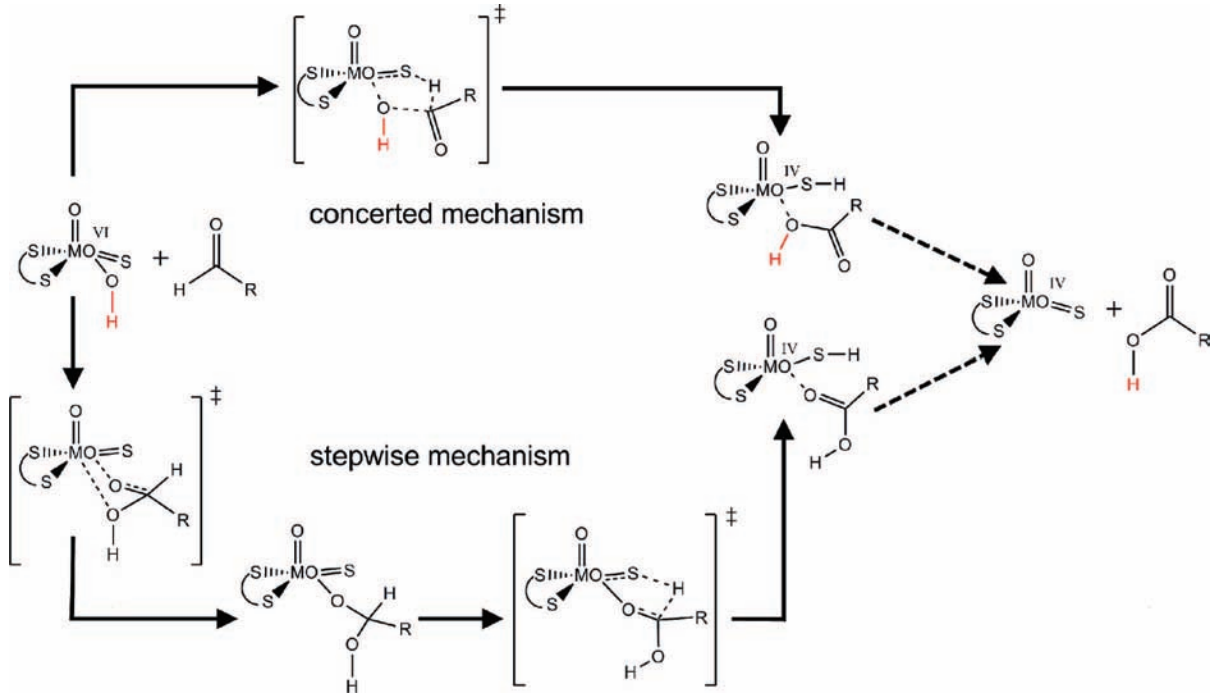

[a](i) protonated cofactor: concerted and stepwise pathways, see refs 9, 10 and 12 (ii) deprotonated cofactor (without proton shown in red): concerted pathway, see ref 13 (stepwise pathway not found).

concerted pathway which treats the nucleophilic attack and hydride transfer as a concomitant process, a lower barrier was obtained (11.9 kcal/mol). Solvent effects were taken into account using the PCM model and were found not to change the preference for the concerted path. However, there is experimental evidence against such a concerted mechanism[12] in the case of the oxidation of xanthine by xanthine oxidase. It is known from isotope-labeling experiments that the labeled oxygen from the Mo−^{18}OH is transferred to the product[18] and that the product is bound via this labeled oxygen, as has been proven in the case of violapterin oxidized by xanthine oxidase.[28]

In a recent study, Amano et al.[13] applied DFT(B3LYP) and correlated ab initio methods up to CCSD(T) to calculate energy profiles using formamide as a substrate. They considered concerted and stepwise mechanisms both for protonated and deprotonated cofactor models. The reported DFT(B3LYP) and CCSD(T) barriers are in the range of 39−42 kcal/mol (concerted/protonated, stepwise/protonated) and 35−38 kcal/mol (concerted/deprotonated), respectively, while a stepwise mechanism with a deprotonated cofactor could not be found. The authors conclude that a one-step mechanism with a deprotonated active site is most plausible.

QM model studies can provide valuable mechanistic insights at the molecular level, but they normally do not include the effects of the protein/solvent environment. This is achieved by QM/MM methods which have become a popular alternative for exploring enzymatic reactions with reasonable accuracy and affordable computational cost.[29] Here we report our recent QM/MM studies on the reductive half-reaction of aldehyde oxidoreductase with acetaldehyde as substrate. We have investigated five possible pathways to compare the concerted and stepwise protocols and to evaluate the importance of Glu869, checking both possible protonation states. Compared with published QM model studies (see above), pathways A and B (with protonated cofactor) have common features with the previously considered concerted and stepwise mechanisms, respectively. No QM equivalents to pathways C-E have been reported so far; a stepwise mechanism with deprotonated cofactor (as in pathway C) has been searched for, but could not be located at the QM level.[13] Our QM/MM calculations suggest that the reductive half-reaction is a three-step process, and support the Lewis base-assisted scheme with deprotonated Glu869 which activates the nucleophilic attack.

2. Methods

Initial coordinates were taken from the X-ray crystal structure[30] (PDB Code: 1VLB, resolution: 1.28 Å) obtained from *Desulfovibrio gigas*. The Mo=OR1 group of the desulfo-form was replaced by Mo=SR1 to prepare the active form. The protonation states of the titratable residues (His, Glu, Asp) were chosen based on the pK_a values given by the empirical PROPKA procedure[31] and verified through visual inspection. The total charge of the whole system was −12e. In addition, we built a neutral system with zero net charge by selectively protonating titrable residues on the surface of the protein. A partial solvation scheme was used to solvate the region of 35 Å around the Mo center by overlaying a water ball on the enzyme. A potential was imposed on the water sphere to prevent the free water molecules from escaping into the vacuum. The

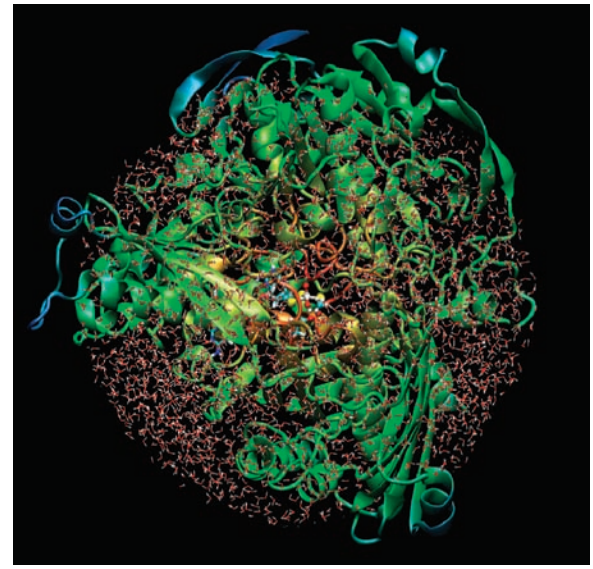

Figure 1. AOR with solvent shell from partial solvation setup.

solvated systems were then relaxed by performing energy minimizations and molecular dynamics (MD) simulations at the MM level using the CHARMM27 force field[32] as implemented in the CHARMM program.[33] During the classical energy minimizations and MD simulations, an active region was defined to include the residues within 20 Å, and the water molecules within 35 Å around the Mo atom. The residues and water outside the active region as well as the non-hydrogen atoms of pterin, the pyrano group (dithio-Mo(=O)(=S)(OH)-ene) and the C=O group of the substrate were fixed. The equilibrated systems (see Figure 1) contained 23357 atoms, including 3237 TIP3P water molecules and 5 ions (two Mg^{2+} and three Cl^-).

The chosen QM/MM methodology is analogous to that used in our previous studies. Here we briefly mention some aspects relevant to the present work. Minimized snapshots from the MD trajectories were taken as the initial structures for QM/MM optimization. In the QM/MM calculations, the QM part was treated by the B3LYP[34−39] density functional method, and the MM part was described by the CHARMM27 force field. An electronic embedding scheme[40] was adopted in the QM/MM calculations, the MM charges were incorporated into the one-electron Hamiltonian of the QM calculation, and the QM/MM electrostatic interactions were evaluated from the QM electrostatic potential and the MM partial charges. No cutoffs were introduced for the nonbonding MM and QM/MM interactions. Hydrogen link atoms with the charge shift model[41,42] were employed to treat the QM/MM boundary. The TURBOMOLE program[43] was used for the QM treatment in the QM/MM

(27) Allen, F.; Kennard, O. *Chem. Des. Autom. News* **1993**, *8*, 31–37.
(28) Hemann, C.; Ilich, P.; Stockert, A. L.; Choi, E. Y.; Hille, R. *J. Phys. Chem. B* **2005**, *109*, 3023–3031.
(29) Senn, H. M.; Thiel, W. *Top. Curr. Chem.* **2007**, *268*, 173–290.
(30) Rebelo, J. M.; Dias, J. M.; Huber, R.; Moura, J. J. G.; Romão, M. J. *J. Biol. Inorg. Chem.* **2001**, *6*, 791–800.
(31) Li, H.; Robertson, A. D.; Jensen, J. H. *Proteins: Struct., Funct., Bioinf.* **2005**, *61*, 704–721.
(32) MacKerell, A. D.; et al. *J. Phys. Chem. B* **1998**, *102*, 3586–3616.
(33) Brooks, B. R.; Bruccoleri, R. E.; Olafson, B. D.; States, D. J.; Swaminathan, S.; Karplus, M. *J. Comput. Chem.* **1983**, *4*, 187–217.
(34) Slater, J. C. *Phys. Rev.* **1951**, *81*, 385–390.
(35) Vosko, S. H.; Wilk, L.; Nusair, M. *Can. J. Phys.* **1980**, *58*, 1200–1211.
(36) Becke, A. D. *Phys. Rev. A* **1988**, *38*, 3098–3100.
(37) Becke, A. D. *J. Chem. Phys.* **1993**, *98*, 5648–5652.
(38) Stephens, P. J.; Devlin, F. J.; Chabalowski, C. F.; Frisch, M. J. *J. Phys. Chem.* **1994**, *98*, 11623–11627.
(39) Lee, C. T.; Yang, W. T.; Parr, R. G. *Phys. Rev. B* **1988**, *37*, 785–789.
(40) Bakowies, D.; Thiel, W. *J. Phys. Chem.* **1996**, *100*, 10580–10594.
(41) de Vries, A. H.; Sherwood, P.; Collins, S. J.; Rigby, A. M.; Rigutto, M.; Kramer, G. J. *J. Phys. Chem. B* **1999**, *103*, 6133–6141.
(42) Sherwood, P.; de Vries, A. H.; Collins, S. J.; Greatbanks, S. P.; Burton, N. A.; Vincent, M. A.; Hillier, I. H. *Faraday Discuss.* **1997**, 79–92.
(43) Ahlrichs, R.; Bär, M.; Häser, M.; Horn, H.; Kölmel, C. *Chem. Phys. Lett.* **1989**, *162*, 165–169.

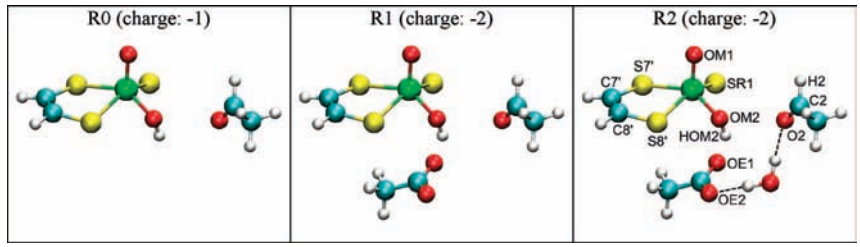

Figure 2. Definition of the QM regions.

calculations. The CHARMM27 force field was run through the DL_POLY program[44] to handle the MM part of the systems. The QM/MM calculations were performed with the ChemShell package[45] that integrates the TURBOMOLE and DL_POLY programs and also performs geometry optimization with the HDLC optimizer.[46]

Three QM regions were adopted in the QM/MM calculations (Figure 2). The QM region R0 represents the simplest model containing only the molybdenum-cofactor model $[Mo(S_2C_2H_2)(=O)(OH)(=S)]^-$ and the substrate acetaldehyde (CH_3CHO). Since the residue Glu869 is conserved within the XO family and essential for the activity of XHD,[47] it is reasonable to include it in the QM part: QM region R1 is obtained from R0 by adding part of the side chain of Glu869 ($-CH_2CO_2^-$). QM region R2 contains an additional water molecule in the active site. For one of the pathways we employ a variant of QM region R1 called R1p with protonated Glu869 ($-CH_2CO_2H$). The total charge of the QM region is -1 for R0 and R1p, and -2 for R1 and R2. The atom labels shown in Figure 2 are taken from the crystal structure 1VLB. Whenever necessary, they will be specified more precisely in the format Resname:AtomName, for example as AALD:O2 for atom O2 in acetaldehyde.

Two basis sets were employed that are defined as follows:

B1: Lanl2DZ[48] + f polarization[49] for Mo, Lanl2DZ[50] + d polarization[51] for S, and 6-31+G**[52,53] for the rest (C, H, O); this is the basis used in ref 12.

B2: Standard def2-TZVP basis set[54] composed of ECP-28-MWB-TZVext[55]+P(f) for Mo, TZV′+P(21/1) for S, TZVPP for C, O, TZP for H.

For QM region R1, B1 and B2 contain 316 and 552 basis functions, respectively. All pathway calculations and optimizations of stationary points were done using basis B1 in combination with the B3LYP hybrid functional. In addition, the stationary points on the energetically favored pathway C were reoptimized using the larger basis B2 in combination with the functionals BP86,[34−36,56,57] BLYP,[34,36,39] B3LYP[34−39] and BHLYP.[34,36,39,58]

In geometry optimizations at the QM/MM level, the active optimized region included the QM region and all residues and water molecules of the MM region within 10 Å around the Mo-center (see Supporting Information for a detailed list). Reaction paths were scanned along suitably defined reaction coordinates by performing constrained optimizations at each point. This provided starting structures for subsequent full optimizations of all relevant stationary points which employed the low-memory Broyden−Fletcher−Goldfarb−Shanno (L-BFGS) algorithm for minima and the partitioned rational function optimizer (P-RFO) for transition states, as implemented in the HDLC code.[46] We ensured by careful reaction path optimization and visual inspection of the optimized structures that the computed stationary points are connected by continuous pathways. Freqency calculations on the QM region confirmed that all reported transition states are characterized by a dominant transition vector that corresponds to the investigated reaction.

3. Results

Our mechanistic studies on aldehyde oxidoreductase at the QM/MM level start from the hydroxide-bound resting state. Five pathways (A−E) were investigated which differ with regard to the interaction between the cofactor and substrate, the mechanistic role and protonation state of Glu869, and the involvement of water. The neutral model system was used to perform the calculations on Pathways A, B, and C, while the charged model was used for Pathways C and D. For Pathway E, we set up a second neutral system with protonated Glu869, starting at the product side with bound acetic acid. All energies values given in this section are QM/MM energies (i.e., including QM, MM, and QM/MM interaction terms), without zero-point and thermal corrections. Unless noted otherwise, these energies were obtained using B3LYP/B1 as QM treatment.

3.1. Pathway A: Concerted Reaction. Pathway A is concerted and similar to the one considered in the QM model system.[12] The reaction proceeds by the simultaneous formation of the C2−OM2 and SR1−H2 bonds (see Scheme 3). The reaction coordinate was therefore defined as $d_{C2-H2}-d_{OM2-C2}-d_{SR1-H2}$. Transition state (TS) optimization gave a barrier of 20.2 kcal/mol using QM region R0. This value is slightly higher than that found in corresponding QM model calculations (18.5 kcal/mol for acetaldehyde[12]) which may be due to the intrinsic constraints of the protein in the active site. Without direct information on the topology of the active site in the substrate-bound enzyme, we rely on the crystal structure of inhibitor-bound enzyme where there are three water molecules helping to anchor the inhibitor through H-bond interactions with the nearby residue Arg501. In our setup, these water molecules are conserved and may be involved in H-bond interactions with the substrate. In fact, on the energy surface for moving acetaldehyde to the cofactor, there is a very shallow region in the beginning until the OM2−C2 distance is around 3 Å (see Supporting Information). The closer approach of acetaldehyde to the cofactor implies some loss of hydrogen bonding with

(44) Smith, W.; Forester, T. R. *J. Mol. Graph.* **1996**, *14*, 136–141.
(45) Sherwood, P.; et al. *J. Mol. Struct. (THEOCHEM)* **2003**, *632*, 1–28.
(46) Billeter, S. R.; Turner, A. J.; Thiel, W. *Phys. Chem. Chem. Phys.* **2000**, *2*, 2177–2186.
(47) Leimkühler, S.; Stockert, A. L.; Igarashi, K.; Nishino, T.; Hille, R. *J. Biol. Chem.* **2004**, *279*, 40437–40444.
(48) Hay, P. J.; Wadt, W. R. *J. Chem. Phys.* **1985**, *82*, 270–283.
(49) Ehlers, A. W.; Böhme, M.; Dapprich, S.; Gobbi, A.; Höllwarth, A.; Jonas, V.; Köhler, K. F.; Stegmann, R.; Veldkamp, A.; Frenking, G. *Chem. Phys. Lett.* **1993**, *208*, 111–114.
(50) Wadt, W. R.; Hay, P. J. *J. Chem. Phys.* **1985**, *82*, 284–298.
(51) Höllwarth, A.; Böhme, M.; Dapprich, S.; Ehlers, A. W.; Gobbi, A.; Jonas, V.; Köhler, K. F.; Stegmann, R.; Veldkamp, A.; Frenking, G. *Chem. Phys. Lett.* **1993**, *208*, 237–240.
(52) Hariharan, P. C.; Pople, J. A. *Theor. Chim. Acta* **1973**, *28*, 213–222.
(53) Clark, T.; Chandrasekhar, J.; Spitznagel, G. W.; Schleyer, P. v. R. *J. Comput. Chem.* **1983**, *4*, 294–301.
(54) Weigend, F.; Ahlrichs, R. *Phys. Chem. Chem. Phys.* **2005**, *7*, 3297–3305.
(55) Andrae, D.; Häussermann, U.; Dolg, M.; Stoll, H.; Preuss, H. *Theor. Chim. Acta* **1990**, *77*, 123–141.
(56) Perdew, J. P. *Phys. Rev. B* **1986**, *33*, 8822–8824.
(57) Perdew, J. P. *Phys. Rev. B* **1986**, *34*, 7406.
(58) Becke, A. D. *J. Chem. Phys.* **1993**, *98*, 1372–1377.

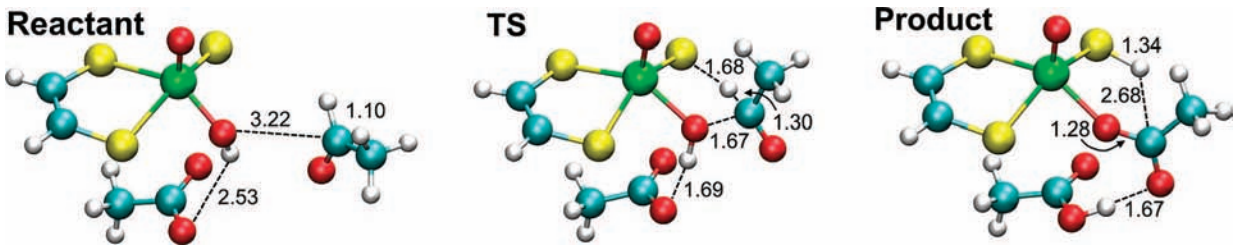

Figure 3. Structures for the concerted pathway from R1/B1 calculations.

Scheme 3. Mechanism of the Concerted Reaction (Total Charge −2)

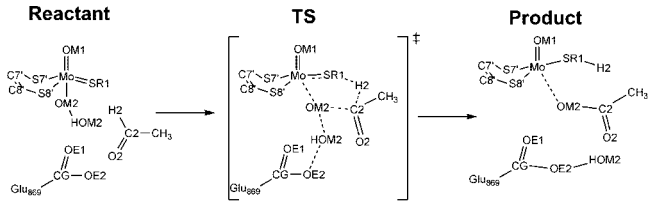

the water molecules which is expected to make a minor contribution to the barrier.

We have also studied the concerted path by including residue Glu869 in the QM region (i.e., using QM region R1) and allowing it to participate in the reaction (see Scheme 3). The calculations on the neutral model predict a barrier of 20.2 kcal/mol which is same as that from R0 calculations. In spite of this similarity, there are differences concerning HOM2. In the reactant, there is an H-bond interaction between Glu869:OE1 and HOM2, which is conserved throughout the R0 calculation. By contrast, in the R1 calculation, this interaction is lost, and HOM2 forms a new bond with Glu869:OE2. The electrostatic effect from Glu869 was examined by setting the point charges in the side chain of Glu869 to zero in an additional R0 test calculation; the barrier was found to increase by about 8 kcal/mol, and the reaction became endothermic by 4 kcal/mol. This clearly demonstrates the stabilizing electrostatic effect of Glu869 on this pathway.

Figure 3 shows the stationary points found at the R1/B1 level. A five-membered ring forms in this phase, and we observe the partial formation of C2−OM2 (1.667 Å) and SR1−H2 (1.683 Å), as well as the partial cleavage of Mo−OM2 (2.070 Å) and C2−H2 (1.298 Å).[59] The Mo=S bond is weakened and is becoming a single bond (2.243 Å). These geometrical changes reflect the concerted nucleophilic attack and hydride transfer (see also the population analysis in Figure S3 of the Supporting Information).

3.2. Pathway B: Initial Dative Bond between Mo and Substrate. Since the Mo atom can generally be penta- or hexa-coordinated, we have considered an alternative pathway B with initial coordination of the substrate. The first step in pathway B is the formation of a dative C2−OM2 bond coupled with the coordination of AALD:O2 to Mo. An intermediate is obtained with OM2 shared by Mo and AALD:C2. Rotation around the C2−OM2 bond then breaks the interaction between Mo and OM2. The last step is the hydride transfer (H2) from acetaldehyde to SR1 (see Scheme 4).

The possible binding of the carbonyl oxygen of aldehyde to molybdenum was proposed in a previous crystallographic study[15] but was characterized as being unfavorable in a recent QM study.[12] We carried out calculations on this pathway to find out whether it can become a possible channel for the oxidation of acetaldehyde when the protein environment is included. As the results with QM regions R0 and R1 are very similar (see Supporting Information), we discuss only the R1 results.

For pathway B, all calculations gave a mechanism in which the nucleophilic attack and hydride transfer happen sequentially. The migration of OM2 to C2 occurs first and an intermediate forms. Hence, we defined the reaction coordinate for formation of the C2−OM2 bond, coupled with the coordination of the carbonyl group (O2) of the substrate to the Mo atom, and the following reorientation of the hydroxide group as d_{Mo-OM2}–d_{OM2-C2}. The final hydride transfer is represented by the reaction coordinate d_{C2-H2}–d_{H2-SR1} and yields the product acetic acid and the cofactor in its reduced form.

In a previous QM study, Wu and Zhang[12] explored the possibility of the formation of a Mo−O dative bond between the cofactor model and formaldehyde, and reported a barrier of 17.8 kcal/mol for the nucleophilic attack. In the QM/MM calculations, the interactions with the surrounding protein environment favor a different orientation of the hydrogen bond network around the hydroxo group, and in addition, the enzyme provides a lipophilic region (Phe425, Tyr535) that further helps to orient the substrate (see Figure S1 in the Supporting Information). This leads to somewhat different transition states: in the QM study, the O2 atom attaches to the Mo atom from the position trans to OM1 (proximal position) to form a distorted octahedral intermediate, while in the QM/MM study, we do not observe any coordination of the substrate from the proximal position where the negatively charged Glu869 is situated and prevents a facile approach of the O2 atom which instead comes in between OM1 and OM2. If we consider the QM/MM transition structure as a distorted octahedron, the O2 atom occupies one equatorial position (in a plane together with S7′,

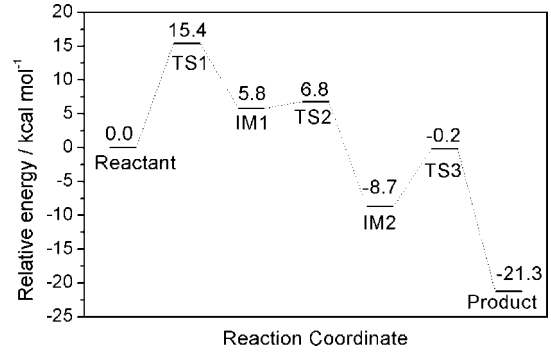

Figure 4. QM/MM energy profile for pathway B from R1/B1 calculations (neutral system).

(59) Smith, P. D.; Slizys, D. A.; George, G. N.; Young, C. G. *J. Am. Chem. Soc.* **2000**, *122*, 2946–2947.

Scheme 4. Mechanism of Pathway B (Total Charge −2)

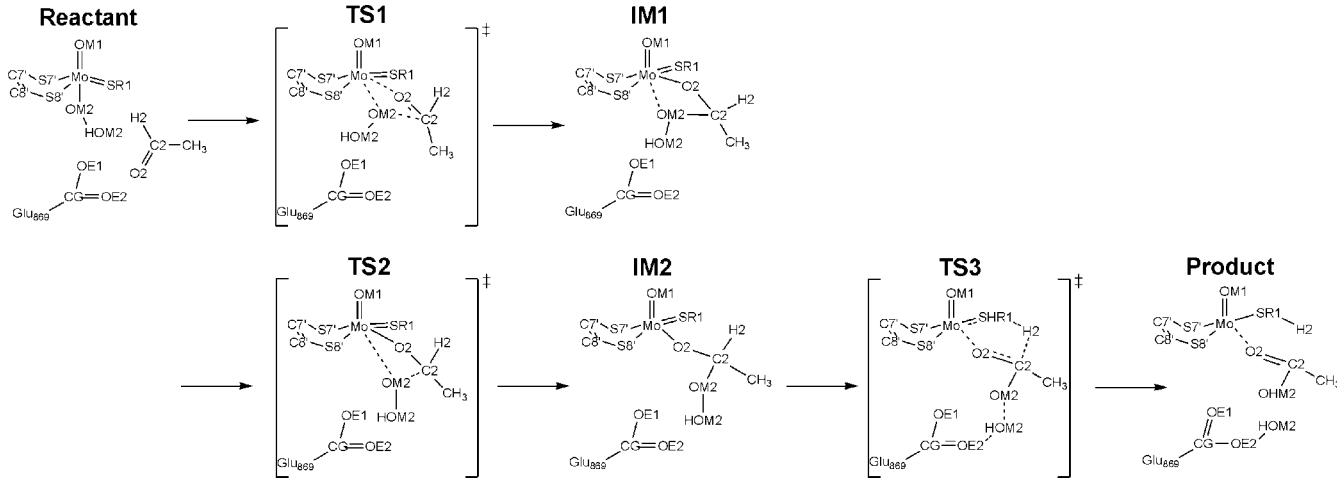

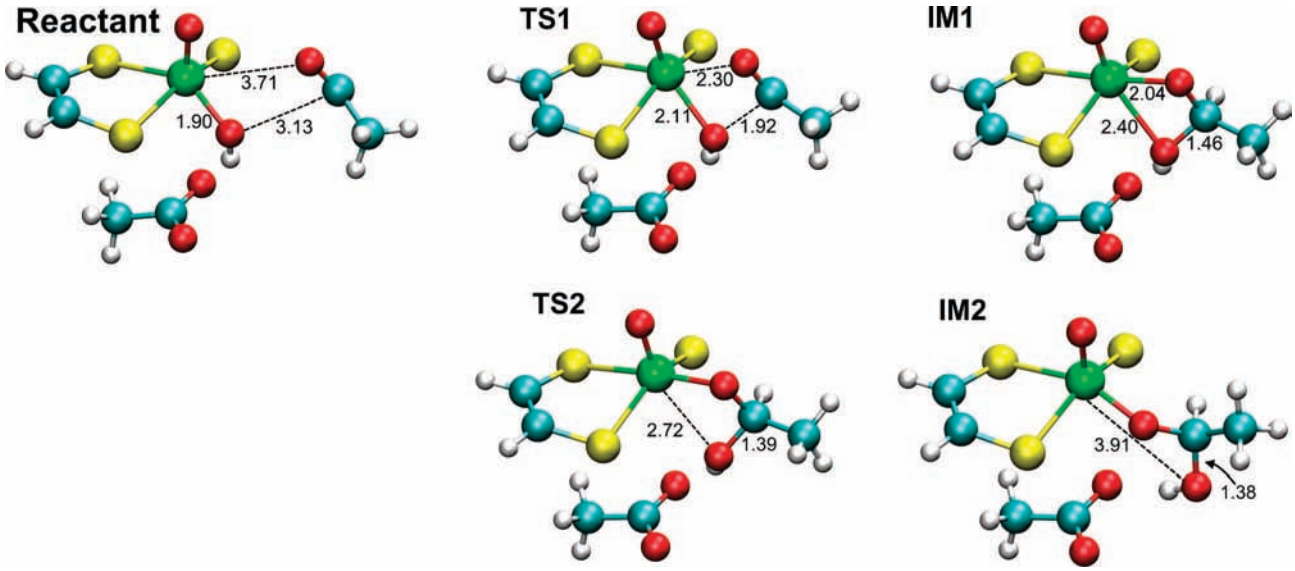

Figure 5. Selected stationary points along pathway B from R1/B1 calculations.

Scheme 5. Difference in the Coordination Pattern for TS1 in QM and QM/MM Work

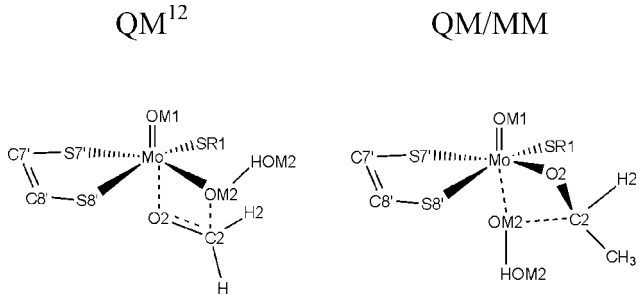

S8′, and SR1), and OM2 moves down to stay on the axis containing the OM1 and Mo atoms. The corresponding structures are shown in Scheme 5.

The energy profile for pathway B is depicted in Figure 4. The initial nucleophilic attack of the hydroxide group (OM2−HOM2) via TS1 has to overcome a barrier of 15.4 kcal/mol. The resulting intermediate (IM1) is a shallow minimum, and the dissociation of the Mo−OM2 bond (i.e., the reorientation of the OM2−HOM2 group) via TS2 requires an activation of only 1.0 kcal/mol. The final hydride transfer via TS3 has a barrier of 8.5 kcal/mol (relative to IM2). The rate-determining barrier of 15.4 kcal/mol for TS1 is lower than the corresponding QM value (21.9 kcal/mol[12]). The overall reaction is exothermic by 21.3 kcal/mol.

Compared to pathway A, the formation of the hexacoordinated molybdenum complex not only guides the reaction to a stepwise mechanism, but also decreases the activation energy significantly. This suggests that the stepwise pathway

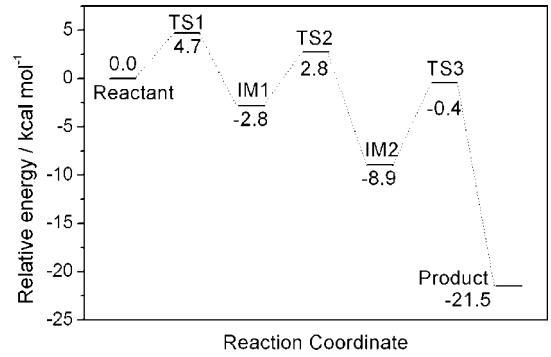

Figure 6. QM/MM energy profile for pathway C from R1/B1 calculations on the neutral model.

Scheme 6. Mechanism of Pathway C (Total Charge −2)

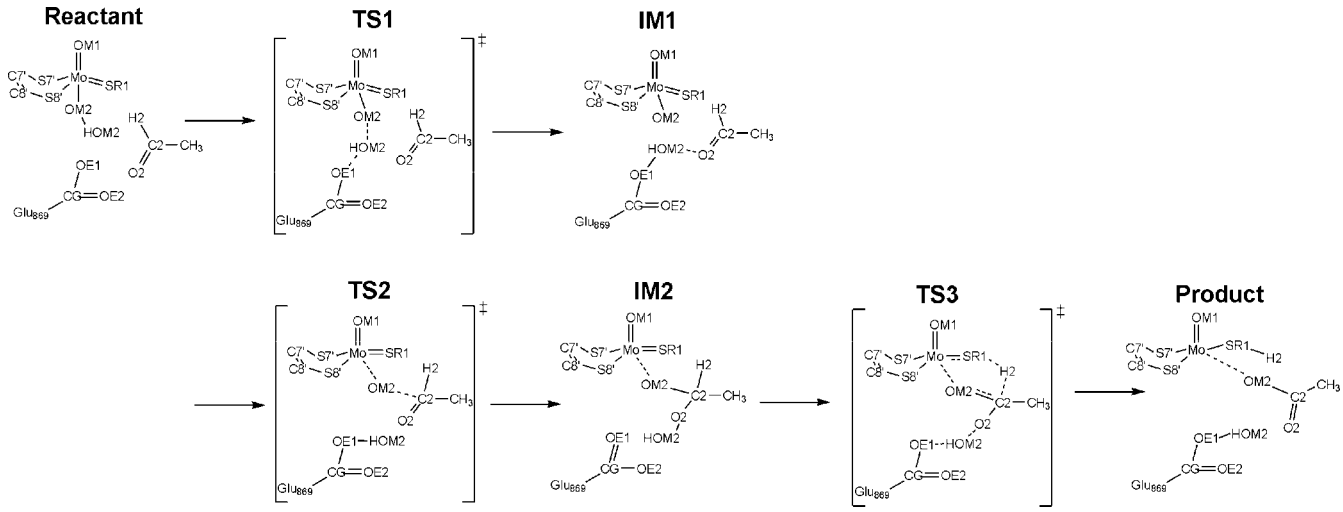

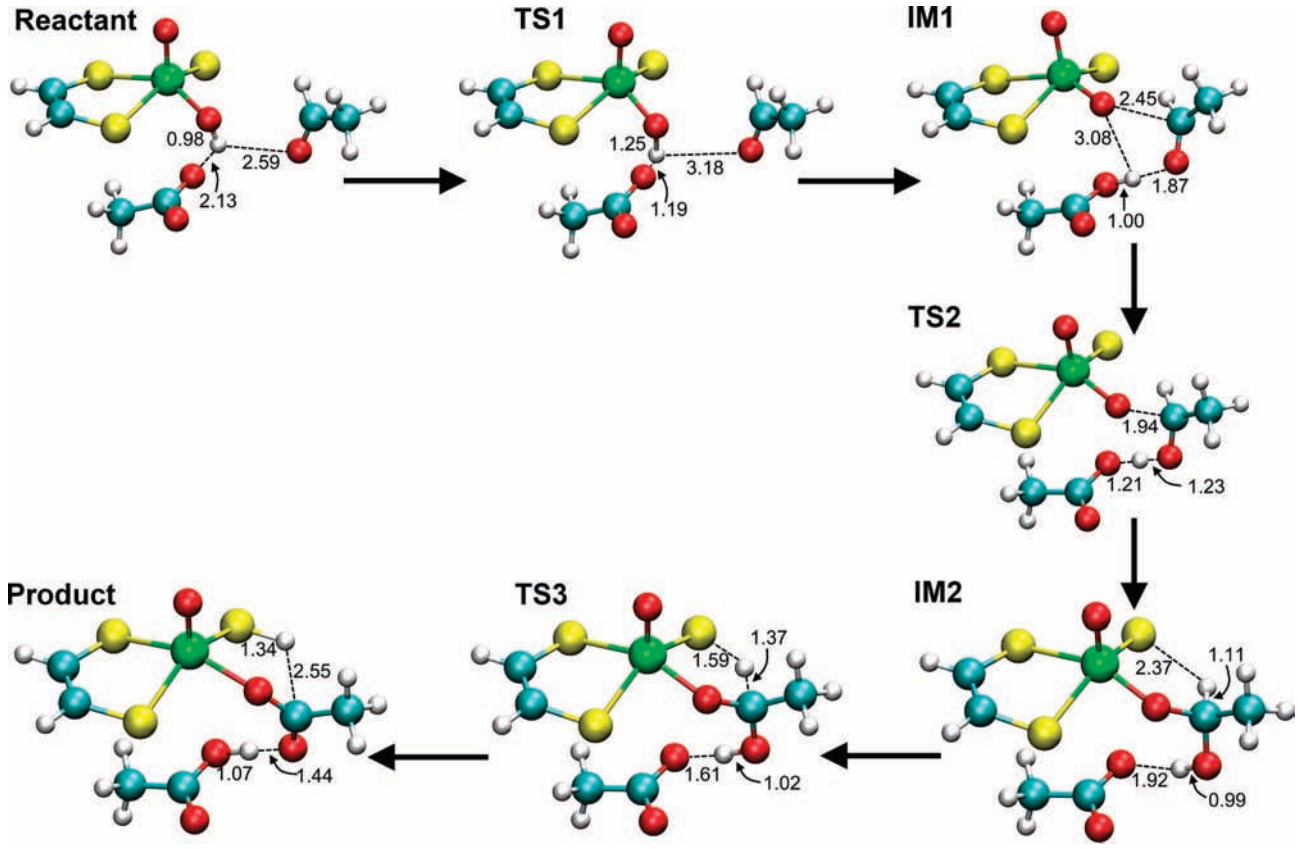

Figure 7. Stationary points along pathway C from R1/B1 calculations.

is more favorable for the reductive half-reaction, with the nucleophilic attack of hydroxide to acetaldehyde being the rate-determining step for this pathway.

Figure 5 shows selected stationary points along this pathway. We can see that in the intermediate (IM2), the OM2−HOM2 group migrates to the target C atom (AALD:C2) of the substrate and the AALD:O2 atom bridges Mo and C2 (distances of 1.901 and 1.448 Å, respectively). After the hydride transfer, the interaction between Mo and O2 is weakened due to the recovery of the C2=O2 double bond.

For each of the pathways A and B considered so far, R0 and R1 calculations (without and with Glu869 in the QM region) gave similar results. This indicates that the role of Glu869 can be equally well described at the MM and QM level in these two mechanistic scenarios where Glu869 serves as an H-bond acceptor. This is no longer true for pathways C and D which involve an initial proton transfer from the Mo-cofactor to Glu869 that acts as a base. The QM/MM calculations for pathways C and D will therefore employ the larger QM regions R1 and R2, respectively.

3.3. Pathway C: Glu869 Promoted Pathway. Pathway C consists of three steps and starts with a proton transfer (HOM2) from the Mo-cofactor to Glu869 prior to the reductive half-reaction. The Glu869:OE1 and AALD:O2

atoms are bridged by the proton (HOM2), and thus there is no coordination between Mo and O2 as observed in Pathway B (see Scheme 6).

A recent mutation study on xanthine dehydrogenase (XDH)[47] indicates that the glutamate (Glu730, corresponding to Glu869 in AOR) is essential for catalysis and may contribute ~10 kcal/mol in stabilizing the transition state. A Lewis base-assisted scheme has been proposed to address the crucial role of glutamate.[60] In the following, we explore this scheme in which a proton transfer step from the Mo-cofactor to the deprotonated Glu869 occurs prior to the nucleophilic attack step.

The current QM/MM calculations suggest that the proton transfer from Mo-cofactor to Glu869 does not happen spontaneously during the formation of the OM2−C2 bond. Hence, to take the catalytic effect of residue Glu869 into account explicitly, we moved the proton PCD:HOM2 to Glu869. This step was found to have a barrier of 4.7 kcal/mol for the neutral model (3.5 kcal/mol for the charged model), and the proton could stay on Glu869 only with the assistance of the H-bond acceptor nearby, the substrate AALD. The proton transfer produces an intermediate (IM1) wherein the Mo-cofactor and AALD are bridged by this proton (HOM2) through H-bond interactions (see Figure 6).

In the intermediate, a new Mo=O bond is formed between Mo and OM2 (1.74 Å, comparable to the axial Mo=OM1 bond) and the oxo-group (OM2) is expected to be more active toward the reaction with acetaldehyde. The calculated barrier for the nucleophilic attack is found to be 5.6 kcal/mol (QM/MM energy relative to IM1, 7.6 kcal/mol for the charged model).

In contrast to the significant activation of the nucleophilic attack step by Glu869, the following hydride transfer is not affected much. The barrier to the hydride transfer in pathway C is calculated to be 8.5 kcal/mol (relative to IM2, 8.6 kcal/mol for the charged model) which is comparable to the values in pathway B. Hence, the main role of Glu869 as a base is to activate the hydroxide addition to the substrate, while it has little effect on the barrier to the hydride transfer. The barrier for the hydride transfer is slightly larger than that for the C2−OM2 bond formation (by 2.9 kcal/mol for the neutral model). Thus, hydride transfer becomes the rate-determining step in pathway C.

Unlike pathways A and B, pathway C involves a two-step proton transfer from OM2 to AALD:O2 in the semiacetal intermediate (IM2). By excluding Glu869 from the QM region, we calculated the direct proton transfer in a single step and obtained a similar exothermicity as for pathway C (−11.2 kcal/mol vs −8.9 kcal/mol) but a much larger barrier of 23.4 kcal/mol. This underlines the crucial mechanistic role of Glu869: the initial proton transfer on pathway C is facile only if it proceeds as a two-step process via an intermediate (IM1) where the proton is "stored" at Glu869.

The semiacetal intermediate (IM2), the precursor for the hydride transfer step, is the same as the one on pathway B. Thus, the QM/MM calculations predict an identical energy profile for the last step in pathways B and C (neutral model).

The optimized geometries along pathway C are similar for the charged and neutral models, and therefore we only show the stationary points obtained from the calculations on the neutral model in Figure 7. As can be seen here, after the proton transfer, the migrated proton HOM2 acts as a bridge to acetaldehyde through an H-bond interaction with OM2 (1.871 Å, IM1). During the nucleophilic attack step, this proton builds a covalent bond with O2 in the semiacetal intermediate (1.232 Å in TS2 and 0.991 Å in IM2) to facilitate the C2−OM2 bond formation. The third step, hydride transfer, has a transition state (TS3) with a five-membered ring (C2−H2: 1.368 Å, H2-SR1: 1.594 Å, Mo-SR1: 2.265 Å, Mo−OM2: 1.972 Å, OM2−C2: 1.345 Å).

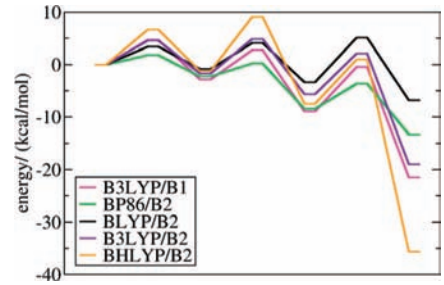

Figure 8. Influence of basis set and functional on energy profile.

Table 1. Calculated QM/MM-Energies in kcal/mol Relative to the Energy of the Reactant for Different Basis Sets and Functionals; Activation Barriers Relative to the Preceding Minima Are Given in Parentheses

	B3LYP/B1	B3LYP/B2	BP86/B2	BLYP/B2	BHLYP/B2
reactant	0.0	0.0	0.0	0.0	0.0
TS1	4.7 (4.7)	4.6 (4.6)	1.8 (1.8)	3.4 (3.4)	6.7 (6.7)
IM1	−2.8	−1.7	−2.3	−0.8	−1.2
TS2	2.8 (5.6)	4.9 (6.6)	0.2 (2.5)	4.1 (4.9)	9.1 (10.3)
IM2	−8.9	−5.6	−8.4	−3.3	−7.5
TS3	−0.5 (8.4)	2.1 (7.7)	−3.6 (4.4)	5.1 (8.4)	1.0 (8.5)
product	−21.5	−19.0	−13.3	−6.8	−35.6

For pathway C we reoptimized all stationary points with basis set B2 and different functionals. Comparing the energy profiles of B3LYP/B1 and B3LYP/B2 (see Figure 8 and Table 1), there is hardly any influence of the enlarged basis set (for details see Supporting Information). Concerning the different functionals, we find the expected behavior for the calculated transition states: the more exact exchange the functional incorporates, the higher are the calculated barriers for TS1 and TS2. TS3 differs from this finding, as the calculated barriers (except the one for BP86) are very similar in energy; in this case, the amount of exact exchange in the functional affects the stability of the resulting Mo(IV) more strongly than the barrier for TS3. For all functionals except BHLYP, hydride transfer via TS3 is the rate-determining step. Overall, the computed reaction profiles are not too sensitive to the choice of basis set or functional, at least in the qualitative sense, which provides justification for using B3LYP/B1 calculations for a consistent comparison of different pathways. We also note in this context, that B3LYP and CCSD(T) results have been found to agree well in a related system.[13]

The results reported here are from calculations on partially solvated models (see section 2). We have also performed calculations on pathway C using a more expensive, fully solvated model which contains 34565 atoms (see Supporting Information for model setup). The computed B3LYP/B1 (B3LYP/B2) barriers are 5.8 (7.3), 2.9 (3.2) and 11.1 (12.4) kcal/mol for proton transfer, nucleophilic attack, and hydride transfer, respectively. They are consistent with the B3LYP results for the partially solvated model (see Table 1).

3.4. Pathway D: Glu869-Promoted Pathway with One Additional Water Molecule. Pathway D is a variant of pathway C with an additional water molecule bridging Glu869 and

(60) Hille, R. *Eur. J. Inorg. Chem.* **2006**, *191*, 3–1926.

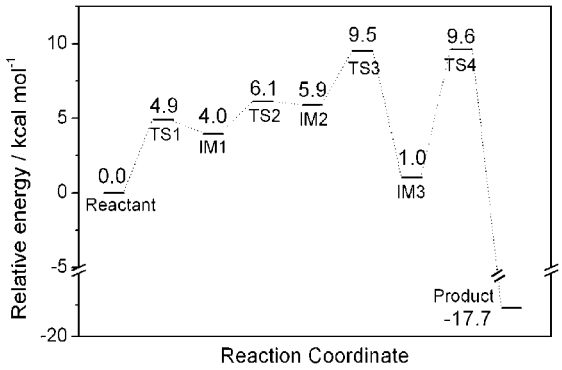

Figure 9. QM/MM energy profile for pathway D from R2/B1 calculations.

AALD, which may facilitate the reaction by a better precoordination of the substrate. The calculations on this pathway explore the possible effect of water present in the active site using the charged model. Classical MD simulations confirm that the additional water molecule remains stable in the active site during a 200 ps MD run (see Figure S11 in the Supporting Information). Due to the similarities in energetics and geometries between the charged and neutral models in pathway C, we did not perform calculations using the neutral model for pathway D.

Following the most favorable protocol found in pathway C, we carefully moved the proton (HOM2) from the cofactor to Glu869. In the calculations on pathway C, an important feature of the first step is the formation of an H-bond between HOM2 and AALD:O2 immediately after the proton transfer which is necessary to assist in the approach of AALD. The presence of one water molecule between Glu869 and AALD does not favor the reorientation of OE1−HOM2 group to form this H-bond. Hence, after the proton HOM2 is delivered to OE1 with a barrier of 4.9 kcal/mol, an additional energy of 2.1 kcal/mol (TS2 in Figure 9) is needed for the corresponding rotation.

Taking advantage of the well-arranged conformation of the active site, the C−O formation becomes a facile process with a barrier of 3.6 kcal/mol. The hydride transfer is the rate-determining step in the reductive half-reaction with a barrier of 8.7 kcal/mol. The whole reaction is exothermic by −17.7 kcal/mol. Hence, with regard to the energetics, pathway D is comparable to pathway C and can be considered as an alternative.

Figure 10 shows selected stationary points of pathway D. In the educt, a water molecule is found between the substrate acetaldehyde and Glu869 acting as an H-bond bridge (distances of 1.820 and 1.739 Å, respectively). This water molecule helps to anchor the substrate, and the H-bond with AALD:O2 may also make AALD:C2 more electrophilic. After the oxidation of the substrate, the water molecule may move up to bind to the Mo atom and thus replenish the oxygen source. The initial proton transfer proceeds via TS1 and produces intermediate IM1 which, due to the presence of the water molecule, has a large distance between HOM2 and AALD:O2 (3.339 Å). The rotation of the OE1−HOM2 group via TS2 leads to a strong HOM2−O2 interaction: the substrate adjusts its orientation such that the HOM2−O2 distance decreases from 2.694 Å in TS2 to 1.676 Å in IM2. In the resulting IM2 conformation, the target atom for the nucleophilic attack, C2, is already quite close to OM2 (2.364 Å) which facilitates the oxygen transfer from molybdenum to C2 (barrier: 3.6 kcal/mol).

3.5. Pathway E: Protonated Glu869. Pathway E is the only one that involves protonated Glu869: Initially, the substrate is rearranged by changes in the H-bond orientation. Afterward, there is a synchronous double proton transfer with concomitant formation of the C2−OM2 bond followed by a hydride transfer (H2) from acetaldehyde to SR1 (see Scheme 7).

In contrast to the previous models, it is not possible to store the HOM2 proton from the cofactor at Glu869:OE1, as the latter residue is already protonated. Therefore, HOE2 has to be transferred at the same time to the substrate, i.e. to AALD:O2. The thus activated substrate concomitantly forms the C2−O2 bond. As there is one additional proton in the QM region, the subsequent hydride transfer, in contrast to all other setups, yields a protonated acetic acid as product. The stationary points are depicted in Figure 11, and the energy profile is shown in Figure 12.

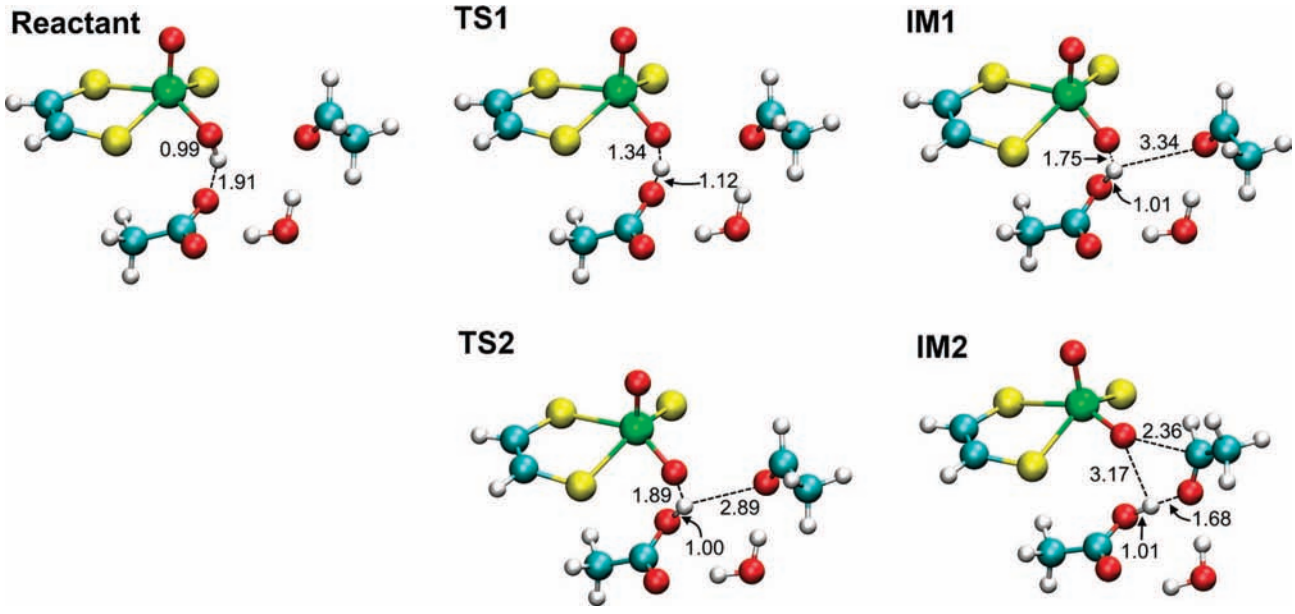

Figure 10. Selected stationary points along pathway D from R2/B1 calculations.

Scheme 7. Mechanism of Pathway E (Total Charge −1)

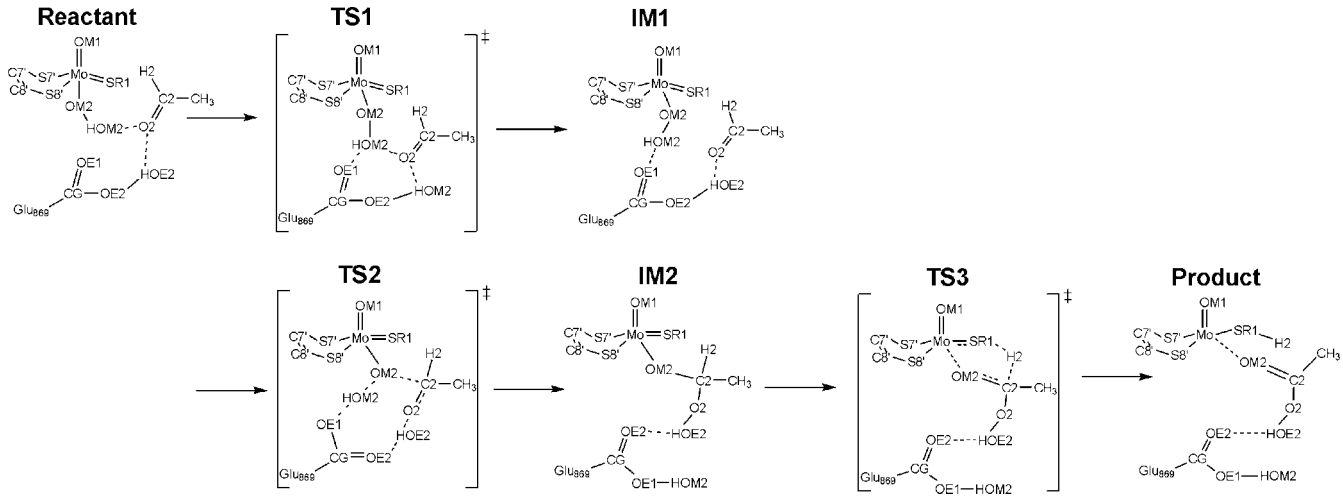

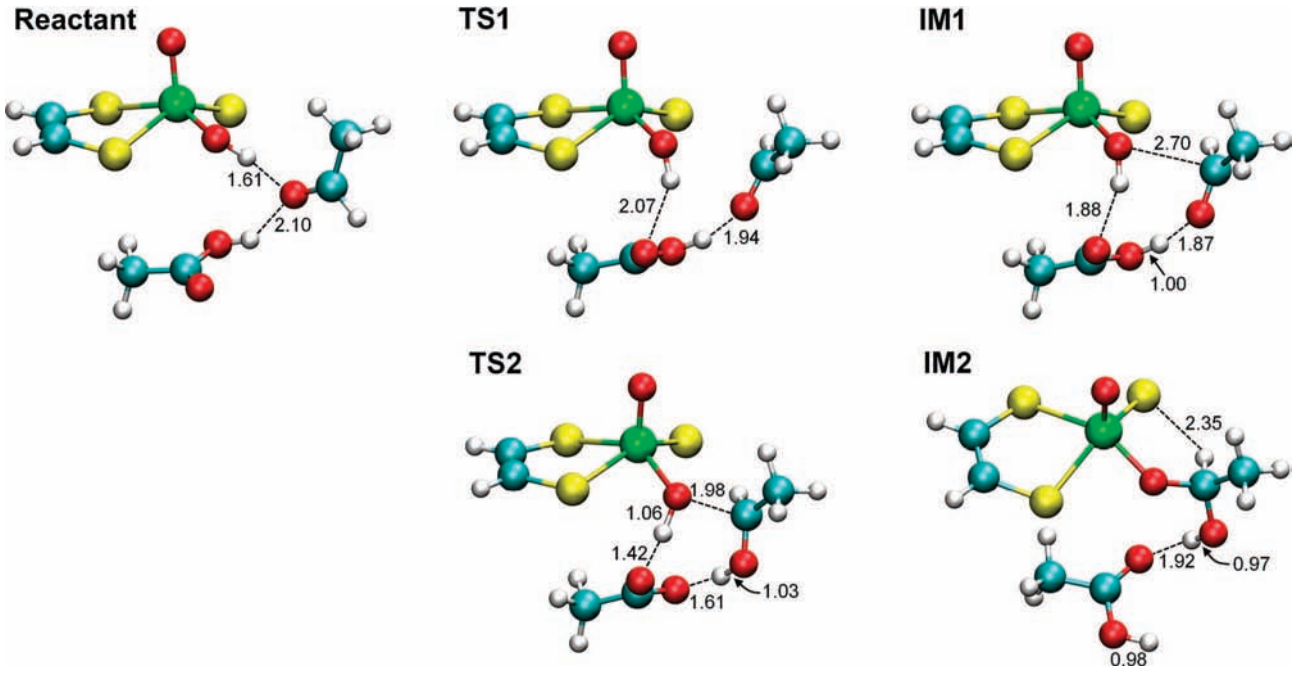

Figure 11. Stationary points along pathway E from R1p/B1 calculations.

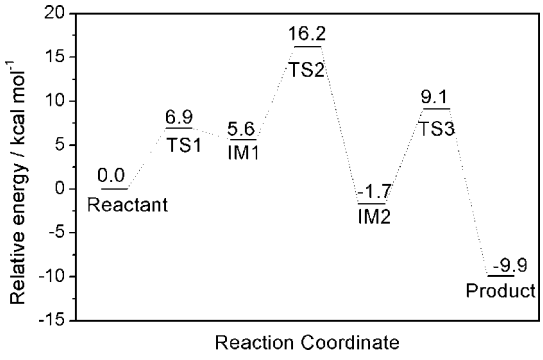

Figure 12. QM/MM energy profile for pathway E from R1p/B1 calculations.

The barrier for such a "double proton transfer" in a single step is rather high. Compared with pathway C (R1 region) there is another complicating feature: In the lowest-lying educt, HOM2 is no longer oriented toward Glu869, but forms a hydrogen bond to the substrate, which leads to a less effective precoordination. The initial phase of the reaction thus involves reorientation of this hydrogen bond (reactant → IM1) as well as C−O bond formation (IM1 → IM2). The effective barrier for this initial phase is 16.2 kcal/mol (see Figure 12) as IM1 resides in a very shallow minimum and is thus in a fast equilibrium with the reactant. For the final hydride transfer (IM2 → product), the barrier of 10.8 kcal/mol for pathway E is just slightly higher than that for pathway C (8.5 kcal/mol). Comparing the rate-determining barriers from the R1/R1p calculations, pathway C is clearly favored over pathway E (8.5 vs 16.2 kcal/mol).

3.6. Pathway C: Mulliken Charges and Fold Angles. In this section we analyze the changes of Mulliken charge distributions and of the puckering of the five-membered ring during the reductive half-reaction of pathway C. The results are similar for the charged and neutral models, and thus we only discuss the former ones to avoid repetition.

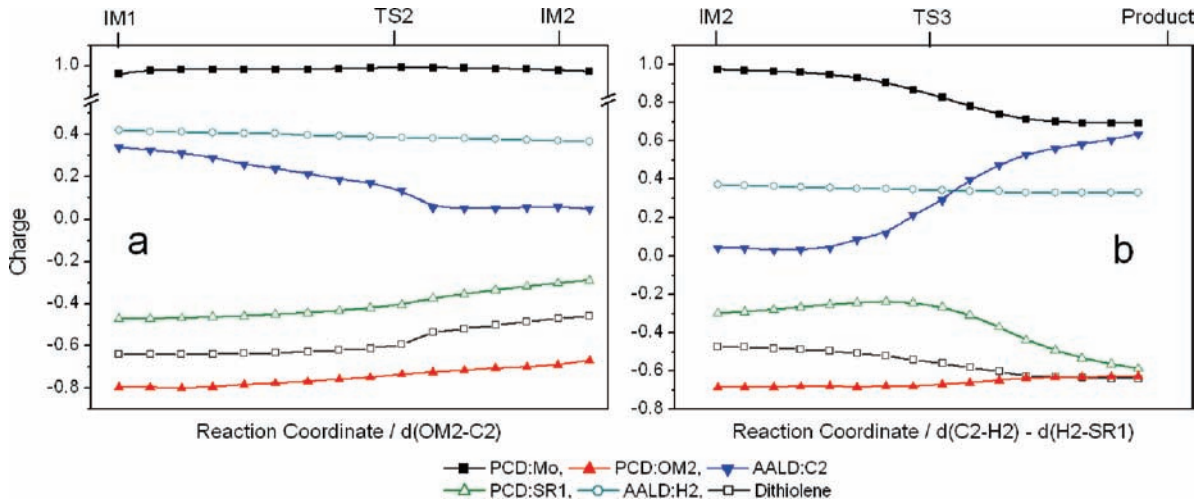

Figure 13. Mulliken charge distributions along pathway C. (Left) C−O formation. (Right) Hydride transfer. The position of the corresponding minima and transition states is indicated (see Scheme 6 and Figure 7).

3.6.1. Partial Charges. In organometallic catalysis, the consumption of the substrate is often accompanied by charge transfer and by a change of oxidation state of the metal center. Hence, monitoring the charge flow may help to characterize redox reactions. The reaction under study involves the formation of a C−O bond (with concomitant weakening of Mo−O) and the dissociation of a C−H bond (coupled to S−H formation). The Mo atom is reduced formally from oxidation state VI to IV, while the substrate (acetaldehyde, AALD) is oxidized. To characterize this charge flow in more detail, Figure 13 shows the change of the partial charges on selected groups (Mo, C2, H2, OM2, SR1, and dithiolene) along pathway C.

In the case of C−O bond formation, the negative charge flows from the Mo-cofactor to the substrate and the target C2 is reduced (see Figure 13a). In the intermediate (IM2 in Figure 7), AALD:O2 receives the proton HOM2 from OE1 and hence becomes part of a hydroxide group. As a result of the accumulation of negative charge on C2, the character of C2 as a base is enhanced upon formation of the C2−OM2 bond which will facilitate the following hydride transfer. For the hydride transfer step (Figure 13b), C2 becomes more acidic when losing the hydrogen atom H2, while Mo and SR1 are reduced. The group charge on the Mo-cofactor becomes more negative which implies a charge transfer concomitant with the migration of H2 from C2 to SR1.

The reduction of the Mo atom also affects the frontier orbitals for the stationary points along the reaction path (Figure 14). In the reactant (oxidized state), the HOMO mainly contains contributions from dithiolene with $\pi_{C=C}$ and sulfur p_z-orbital components (denoted as $\pi_{C=C}$ - p_z(S7′) - p_z(S8′)), and the LUMO is essentially an antibonding combination of the Mo in-plane d-orbital and the p-orbital of SR1 (denoted as d_{xy}(Mo) - p_x(SR1)). In the product (reduced state), the d_{xy}-orbital of Mo is occupied due to the reduction of Mo atom. This is consistent with a study on model compounds.[61] The frontier orbitals of the intermediates, IM1 and IM2, have similar composition as those of the reactant, and are thus not shown.

It has been proposed that the reduction of Mo is possibly a Michaelis-like process through two single-electron steps[62] via a radical intermediate (formed by hydrogen rather than hydride transfer). However, a later experimental study on the reduction potential[63] using different substrates did not support such an assumption. We have tried to locate a radical intermediate (open-shell singlet), which could further be reduced from Mo(V) to Mo(IV) by a one-electron transfer along the Mo−O2 dative bond. The calculation produced a closed-shell compound and thus did not provide any evidence for an open-shell singlet. This gives indirect support to the concerted two-electron reduction of Mo atom.

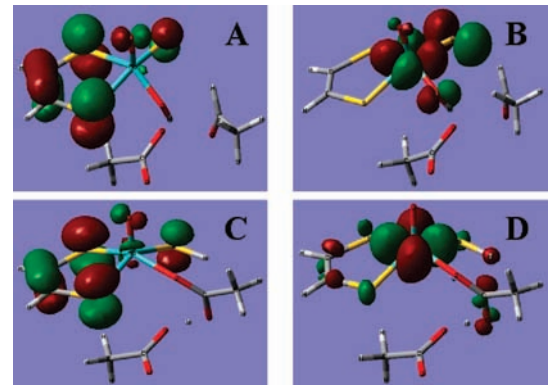

Figure 14. Frontier orbitals for reactant and product from the charged model: Reactant: (A) HOMO. (B) LUMO. Product: (C) HOMO-1. (D) HOMO.

3.6.2. Fold Angle. Another issue is the puckering of the Mo-dithiolene ring. The conformation of the dithiolene subunit has been observed to be slightly different in the oxidized and reduced states both in model compounds[64] and in the enzyme.[15] Enemark and co-workers[61,65,66] suggested that the dynamic variation of this unit may modulate the nucleophilic attack of the hydroxide group to the substrate and the following hydride transfer.

The fold angle (see Scheme 8) was monitored along pathway C (Figure 15). It increases upon C−O formation (by ∼3°) and decreases again during the hydride transfer. This is not surprising when considering the trends in the partial charges on the reactive moiety (Figure 13): the changes in the fold angle are such that they help the cofactor to adapt to the changes in the charge distributions. The dithiolene ligand is an electron-rich group and can act as a "buffer" for

electrons. During C−O bond formation, the flow of electron density from Mo to C2 is compensated by additional interactions between p_z-orbitals of the sulfur atoms of the dithiolene-ligand (S7′ and S8′) and the empty d_{xy}-orbital of Mo (see Figure 14) which are strengthened by increasing the fold angle of the dithiolene ring.[61] By contrast, during the hydride transfer, the positive charge on the cofactor is partially neutralized, and the dithiolene now can recover its original conformation. The more planar structure of the dithiolene helps to delocalize the negative charge flowing to Mo from the Mo=SR1 bond during the hydride transfer. As the d_{xy}-orbital has become the HOMO, the interactions with the p_z-orbitals of the sulfur atoms of the dithiolene become repulsive, and the fold angle decreases.

4. Discussion

Our QM/MM results for the preferred pathway C suggest that Glu869 acts as Lewis base to deprotonate the labile hydroxide ligand and thus to activate the cofactor for nucleophilic attack at the substrate followed by hydride transfer. The oxidation of the substrate in the enzyme is thus predicted to be a Lewis base-catalyzed stepwise process.

In comparison with recent QM model studies, we note that Amano et al.[13] also favor a scenario where the reaction proceeds via a deprotonated cofactor; however, with formamide as substrate they only find a concerted pathway with a high barrier of ca. 35 kcal/mol, whereas QM/MM calculations with acetaldehyde as substrate yield a much more facile stepwise mechanism via a semiacetal intermediate that is stabilized by the electrostatic interaction with the environment. The structure of the intermediate and some features of our preferred pathway C are reminiscent of the stepwise mechanism with a protonated cofactor reported by Zhang and Wu;[12] however, in their QM model study, the stepwise mechanism is less favorable than the concerted one, contrary to the present QM/MM results. Generally speaking, the published QM model studies have not included the Glu869 residue which plays a crucial mechanistic role according to our QM/MM results and the experimental evidence for XHD.[47] Inclusion of Glu869 may pose problems at the QM level since this will create a dianionic QM model system, with strong repulsion between the two negatively charged entities (cofactor and Glu869), which may necessitate the use of geometric constraints. By contrast, such situations are handled quite naturally at the QM/MM level which properly accounts for the stabilization of charged active-site species by the protein environment.

5. Conclusion

The current QM/MM calculations aim at understanding the reaction mechanism in aldehyde oxidoreductase, in particular the catalytic effect of Glu869. Comparison among pathways A, B, and C suggests that Glu869 plays a crucial role as a Lewis base which promotes the cofactor to a more active species. The QM/MM calculations indicate that the energetics of the oxidation of acetaldehyde change significantly when Glu869 is allowed to act as a Lewis base. By deprotonating the labile hydroxide group, Glu869 facilitates C−O bond formation by nucleophilic attack of the oxy-anion on the substrate, and the subsequent hydride transfer becomes the rate-determining step. The benefits from the proton transfer prior to the C−O bond formation are 2-fold: (a) the OM2 atom becomes more basic and hence its nucleophilicity increases; (b) the formation of an H-bond between HOM2 and O2 after the proton transfer perturbs the C2=O2 bond and induces an electron flow to O2, which makes C2 more electrophilic.

Scheme 8. Fold Angle α Is Defined by Three Points: Mo, the Center of S7′ and S8′, and the Center of C7′=C8′

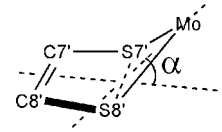

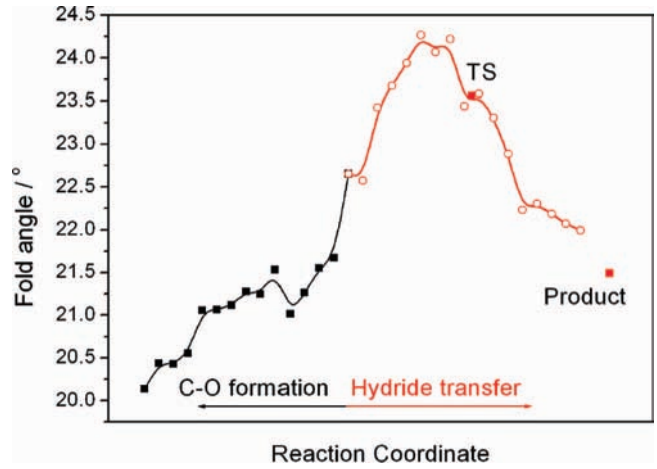

Figure 15. Fold angle along pathway C.

Two alternative scenarios based on pathway C have been considered for the reductive half-reaction. In pathway D there is an additional water molecule between Glu869 and acetaldehyde which may help to position the substrate and may move to the Mo center after the oxidation of the substrate, in order to facilitate product release and to act as oxygen source for the next turnover. The QM/MM energy profiles are similar for pathways C and D so that both seem feasible, with a slight edge for pathway C. By contrast, pathway E is less favorable. It involves a protonated Glu869 (unlike A−D) which precludes the activation of the cofactor by Glu869 acting as a Lewis base (as in C and D), and the computed effective barrier for pathway E is thus significantly higher than those for pathways C and D.

In summary, our QM/MM calculations describe the oxidation of acetaldehyde by the AOR enzyme as a Lewis base-catalyzed stepwise process. The initial deprotonation of the cofactor by Glu869 initiates a nucleophilic attack at the substrate followed by hydride transfer. We are not aware of any detailed experimental studies of this mechanism in AOR. Our QM/MM results are consistent with experimental evidence in related enzymes, i.e., on the crucial role of a nearby Glu residue in xanthine dehydrogenase[47] and oxygen isotope labeling in xanthine oxidase.[18,28] We hope that our

(61) Joshi, H. K.; Enemark, J. H. *J. Am. Chem. Soc.* **2004**, *126*, 11784–11785.
(62) Page, C. C.; Moser, C. C.; Chen, X. X.; Dutton, P. L. *Nature* **1999**, *402*, 47–52.
(63) Stockert, A. L.; Shinde, S. S.; Anderson, R. F.; Hille, R. *J. Am. Chem. Soc.* **2002**, *124*, 14554–14555.
(64) Stiefel, E. I.; Miller, K. F.; Bruce, A. E.; Corbin, J. L.; Berg, J. M.; Hodgson, K. O. *J. Am. Chem. Soc.* **1980**, *102*, 3624–3626.

current QM/MM predictions will trigger corresponding experimental studies in AOR.

Acknowledgment. We thank Prof. Yun-Dong Wu for suggesting this project and for valuable discussions. This work was supported by the Max-Planck-Gesellschaft. S.M. thanks the Fonds der Chemischen Industrie for a Kekulé scholarship.

(65) Joshi, H. K.; Cooney, J. J. A.; Inscore, F. E.; Gruhn, N. E.; Lichtenberger, D. L.; Enemark, J. H *Proc. Natl. Acad. Sci. U.S.A.* **2003**, *100*, 3719–3724.
(66) McNaughton, R. L.; Helton, M. E.; Cosper, M. M.; Enemark, J. H.; Kirk, M. L. *Inorg. Chem.* **2004**, *43*, 1625–1637.

Supporting Information Available: Technical details on system preparation and QM/MM setup. Energy scans, charge distributions, MD results, and detailed numerical data. Complete refs 32 and 45. This material is available free of charge via the Internet at http://pubs.acs.org.

JA805938W